Superconducting transitions in flat-band systems

V. I. Iglovikov,[1] F. Hébert,[2] B. Grémaud,[3,4,5,6] G. G. Batrouni,[2,5,7] and R. T. Scalettar[1]
[1]*Physics Department, University of California, Davis, California 95616, USA*
[2]*INLN, Université de Nice–Sophia Antipolis, CNRS; 1361 route des Lucioles, 06560 Valbonne, France*
[3]*Merlion MajuLab, CNRS-UNS-NUS-NTU International Joint Research Unit UMI 3654, Singapore*
[4]*Laboratoire Kastler Brossel, Ecole Normale Supérieure CNRS, UPMC; 4 Place Jussieu, 75005 Paris, France*
[5]*Centre for Quantum Technologies, National University of Singapore, 3 Science Drive 2, Singapore 117543, Singapore*
[6]*Department of Physics, National University of Singapore, 2 Science Drive 3, Singapore 117542, Singapore*
[7]*Institut Universitaire de France, 103, Boulevard Saint-Michel, 75005 Paris, France*
(Received 30 April 2014; revised manuscript received 5 August 2014; published 11 September 2014)

The physics of strongly correlated quantum particles within a flat band was originally explored as a route to itinerant ferromagnetism and, indeed, a celebrated theorem by Lieb rigorously establishes that the ground state of the repulsive Hubbard model on a bipartite lattice with an unequal number of sites in each sublattice must have nonzero spin S at half filling. Recently, there has been interest in Lieb geometries due to the possibility of topological insulator, nematic, and Bose-Einstein condensed (BEC) phases. In this paper, we extend the understanding of the attractive Hubbard model on the Lieb lattice by using determinant quantum Monte Carlo to study real space charge and pair correlation functions not addressed by the Lieb theorems. Specifically, our results show unusual charge and charge transfer signatures within the flat band, and a reduction in pairing order at $\rho = 2/3$ and $\rho = 4/3$, the points at which the flat band is first occupied and then completely filled. We compare our results to the case of flat bands in the Kagome lattice and demonstrate that the behavior observed in the two cases is rather different.

DOI: 10.1103/PhysRevB.90.094506 PACS number(s): 74.20.−z, 03.65.Vf, 74.62.Bf, 75.10.Jm

I. INTRODUCTION

The form of the electronic dispersion relation $\epsilon(k)$ in the absence of interactions plays a fundamental role in how correlations drive the formation of ordered phases. Qualitative pictures like the Stoner criterion for ferromagnetism simplify the input from $\epsilon(k)$ and focus on the density of states at the Fermi level $N(E_F) = \sum_k \delta[E_F - \epsilon(k)]$. More refined treatments like the random phase approximation (RPA) capture phenomena such as the degree of Fermi surface nesting and provide insight into how the noninteracting susceptibility determines the renormalized response of the system. Both density of states and nesting issues come into play in cuprate superconductivity: Nearest-neighbor hopping on a two-dimensional square lattice such as that occupied by the copper atoms of the CuO_2 sheets has a van Hove singularity in the density of states at half filling which was suggested to lead to an enhanced superconducting critical temperature [1]. Likewise nesting of the Fermi surface with wave vector $\mathbf{q} = (\pi,\pi)$ provides a natural weak-coupling explanation for the antiferromagnetic phase of the undoped parent compounds, complementing the strong-coupling Heisenberg picture. Nesting can also further increase the pairing transition temperature [2].

While the single-band Hubbard model on a square lattice has received the most attention in modeling the cuprates, considerable interest has also focused on the more accurate three-band picture which includes not only the square lattice of copper d orbitals but also the intervening oxygen p orbitals [3–8]. If hopping is restricted to nearest neighbors, this arrangement of sites is bipartite, with, however, unequal numbers $N_p = 2N_d$. In such situations, Lieb showed [9] that, at half filling and with repulsive interaction, the hopping Hamiltonian $\hat{T}$ has a ground state with nonzero spin, $S = (N_p - N_d)/2$. The key element of the physics of such "Lieb lattices" is that the spectrum of $\hat{T}$ consists of $2N_d$ eigenvalues in $+/-$ pairs, separated by a flat electronic band $\epsilon(k) = 0$ with $N_p - N_d$ levels. Figure 1(a) shows an example of a Lieb geometry ($N_p = 2N_d$). While this structure is similar to the CuO_2 planes of the high temperature superconductors, in a realistic cuprate model there is an energy difference between the copper d and oxygen p orbitals. The zero energy modes of $\hat{T}$ can be easily understood: A one particle state formed by creating fermions on the four oxygen sites surrounding the center of any copper plaquette, $|\psi\rangle = (c_1^\dagger - c_2^\dagger + c_3^\dagger - c_4^\dagger)|\text{vac}\rangle$, satisfies $\hat{T}|\psi\rangle = 0$ because hops from the oxygens onto the coppers cancel. This "topological" localization was emphasized earlier by Sutherland [10].

The Lieb lattice, as realized in CuO_2 planes of the cuprate superconductors, was investigated by Varma for possible staggered current phases which might explain pseudogap behavior [11]. Behavior tied to the presence of a flat band [12–20] includes a quantum spin Hall effect driven by spin-orbit coupling and topological phase transitions, e.g., caused by next-nearest-neighbor hopping [21]. Other "decorated" geometries exhibit flat bands, e.g., the Kagome lattice, and are similarly under investigation [22,23], a key difference being the frustrated nature of the Kagome lattice. We compare results obtained for the Lieb lattice to the Kagome lattice and show the results we find are not generic to arbitrary flat-band systems.

In this paper we address two important questions left open by Lieb's theorems [1]: What are the natures of the charge and superconducting response functions [2]? What are the implications of the absence of a minimum in $\epsilon(k)$ for superconductivity (SC) or BEC in a flat band? It has been suggested that the presence of interactions renormalizes the flat band and induces an effective minimum so that BEC can still occur [24] or that the infinite density of states in

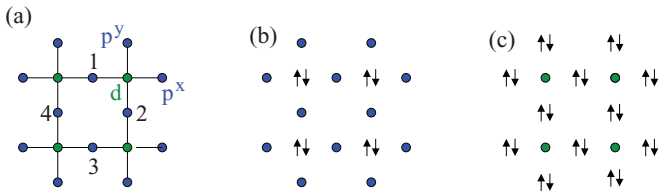

FIG. 1. (Color online) An example of a Lieb lattice, a bipartite geometry with unequal numbers of sites in the two sublattices. (a) The three-band model of the CuO_2 planes of the cuprate. In the case of attractive interactions CDW patterns emerge at two-thirds (b) and four-thirds (c) fillings by doubly occupying the copper or oxygen sublattices, respectively. Localized states form from linear combinations of creation operators on sites 1,2,3,4 (panel a) with alternating phases.

the flat band favors the emergence of SC or other kinds of order [25–27], however no exact numerical work has addressed these issues. Next-generation optical lattice emulation (OLE) experiments have generated Lieb lattice geometries [28,29] and might be able to study this question for bosonic atoms [30]. The attractive fermion Hubbard model (AHM) considered here develops superconducting phases at low temperatures—a BCS phase at weak coupling and BEC pairing at strong coupling [31], with a crossover between these two extreme cases. On lattices which do not have special features in their densities of states [25,26], and in sufficiently high dimension, the BCS limit is characterized by pairs with large sizes ξ and a transition temperature $T_c \sim t\exp[-at/|U|] \sim t\exp[-b/UN(E_{\rm fermi})]$. In the BEC limit, ξ is of the order of a few lattice spacings and $T_c \sim t^2/|U|$, the effective hopping of the tightly bound pairs. We will concentrate on intermediate and large coupling cases ($|U| \geqslant 4$). This is closer to the BEC limit, and hence to possible experiments on bosonic atoms. Furthermore, it is easier to reach the condensation temperature in this case.

II. CALCULATIONAL APPROACH

We consider the AHM on a CuO_2 geometry [Fig. 1(a)].

$$H = -t\sum_{i\alpha\sigma}\left(d^\dagger_{i\sigma}\,p^\alpha_{i\sigma} + d^\dagger_{i+\alpha\,\sigma}\,p^\alpha_{i\sigma} + \text{H.c.}\right) - |U|\sum_{i\alpha}\left[\left(n^d_{i\uparrow}-1/2\right)\left(n^d_{i\downarrow}-1/2\right) + \left(n^{p\alpha}_{i\uparrow}-1/2\right)\left(n^{p\alpha}_{i\downarrow}-1/2\right)\right] \quad (1)$$

We have adopted the notation of the three-band model of the cuprates where the operators $d^\dagger_{i\sigma}$ ($d_{i\sigma}$) create (destroy) fermions on site i of spin σ in a square lattice of copper d orbitals and $p^{\alpha\dagger}_{i\sigma}$ ($p^\alpha_{i\sigma}$) do the same for oxygen p orbitals on the intervening links in the $\alpha = \hat{x},\hat{y}$ directions. Number operators are denoted by $n^{p\alpha}_{i\sigma}$ and $n^d_{i\sigma}$. t is the scale of kinetic energy which we set to unity and $|U|$ is the magnitude of the on-site attraction. N denotes the total number of sites of the lattice [32].

In order to determine the properties of the AHM on a Lieb lattice, Eq. (1), we use determinant quantum Monte Carlo (DQMC) [34,35]. The approach exactly solves the Hamiltonian on lattices of finite size [36]. We present results for up to 6×6 unit cells (108 sites). The absence of the sign problem in the attractive case, $U<0$, allows simulations over a wide range of fillings. We focus our attention on the densities on the d and p orbitals, n^d and $n^{px} = n^{py}$, and on intra-unit-cell (i.e., nearest-neighbor and next-nearest-neighbor) density-density correlations, $\langle n^d n^{px}\rangle$ and $\langle n^{px} n^{py}\rangle$. The total density per site $\rho = \frac{1}{3}(n^d + n^{px} + n^{py})$. We also report data for the local moment $\langle m^2\rangle = \sum_{i\nu}\langle (n_{i\nu\uparrow} - n_{i\nu\downarrow})^2\rangle$ and s-wave pair structure factor $P_s = 1/N^2\ \sum_{i,j,\mu,\nu}\langle B_{i\mu}B^\dagger_{j\nu}\rangle$. Here $B^\dagger_{j\nu}$ creates a pair of up/down spin fermions on site j and orbital $\nu = d, p^x, p^y$. In the definitions of $\langle m^2\rangle$ and P_s the sums are over all N lattice sites (i.e., over both d and p orbitals).

We complement these DQMC calculation with mean field theory (MFT). In this approach, on each site, the attractive interaction is written in term of the operators

$$\Delta_x = \frac{1}{2}(c^\dagger_\uparrow c^\dagger_\downarrow + c_\downarrow c_\uparrow)\quad \Delta_y = \frac{1}{2i}(c^\dagger_\uparrow c^\dagger_\downarrow - c_\downarrow c_\uparrow)$$
$$\Delta_z = \frac{1}{2}(n_\uparrow + n_\downarrow - 1), \quad (2)$$
$$-|U|(n_\uparrow - 1/2)(n_\downarrow - 1/2) = -2|U|\vec{\Delta}\cdot\vec{\Delta}/3 + |U|/4.$$

The vector $\vec{\Delta} = (\Delta_x, \Delta_y, \Delta_z)$ is obtained from the usual spin operator by a particle-hole transformation for the down spin. The mean field decoupling corresponds to approximating, on each site, the interaction term $\vec{\Delta}\cdot\vec{\Delta}$ by $2\langle\vec{\Delta}\rangle\cdot\vec{\Delta}$, leading to three mean field parameters $\langle\vec{\Delta}\rangle$. For repulsive interaction, this decoupling is the analog of the usual SU(2) decoupling in the spin channels [37]. The values $\langle\vec{\Delta}_i\rangle$ are determined by minimizing the free energy.

Both techniques work in the grand canonical ensemble, which could cause a problem when trying to access a given density in the partially filled flat band. This is not the case as the flat band acquires a width due to interactions in the exact DQMC treatment and as the SU(2) symmetry allows us to circumvent this problem in the MF approximation (see below).

III. NUMERICAL RESULTS

A. Local density response

We begin by showing the changes in the occupations $\langle n^d\rangle$ and $\langle n^{px}\rangle = \langle n^{py}\rangle$ on the individual orbitals as the total density ρ increases (Fig. 2). In the noninteracting limit, $\partial\langle n^\alpha\rangle/\partial\rho$ must be nonnegative, and we observe this. However, for $U\neq 0$ we see that the d occupation decreases with increasing ρ. We interpret this in terms of a transition from the $\rho = 2/3$ CDW [Fig. 1(b)] to the $\rho = 4/3$ CDW [Fig. 1(c)]. U favors doubly occupied sites, but to second order in perturbation theory such paired sites are lower in energy by $2t^2/|U|$ for each empty adjacent site. At low densities (double) occupation of the four-fold coordinated d orbitals is favored, but as ρ exceeds 2/3 it becomes advantageous to occupy the more numerous p orbitals and empty the d band.

We emphasize an important feature of CDW patterns on this lattice: Because the d and p sites are inequivalent, there

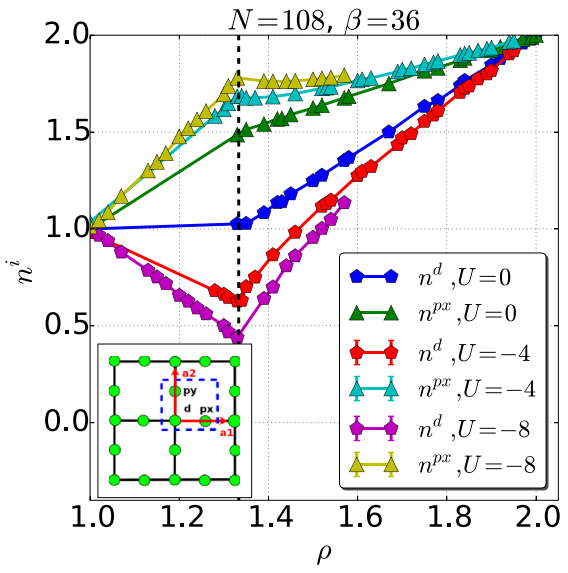

FIG. 2. (Color online) Occupations of the copper (n^d) and oxygen ($n^{p\alpha}$) orbitals as a function of density ρ for $U = 0, -4, -8$. Nonzero attractive interactions induce an unusual charge transfer effect in which the copper occupation decreases even while the overall lattice density increases, with cusps at the endpoint of the filling of the flat band, $\rho = 4/3$. Here and in subsequent figures we show only densities $\rho \geqslant 1$ since our model Eq. (1) is particle-hole symmetric.

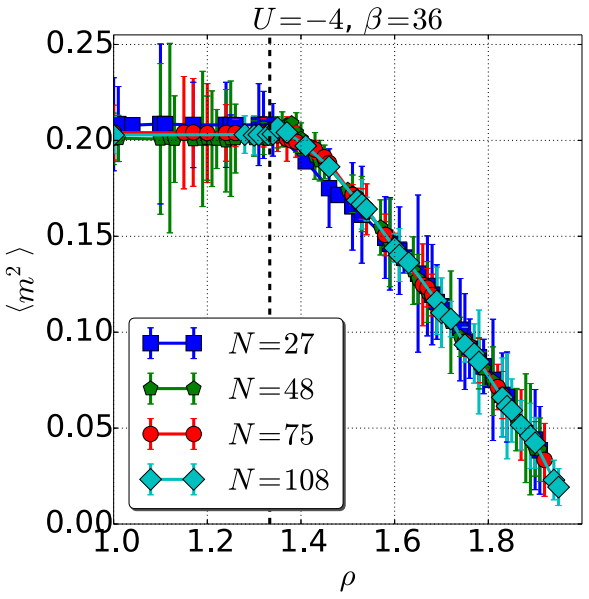

FIG. 3. (Color online) The local magnetic moment $\langle m^2 \rangle$ versus density. $\langle m^2 \rangle$ is constant within the flat band, and then drops for densities $\rho > 4/3$. Here $U = -4t$ and $\beta = 36$. The constant value of $\langle m^2 \rangle$ can be explained within MFT to be a consequence of the SU(2) invariance at $\mu = 0$, see the text for more details.

is a "trivial" difference in charge densities which does not reflect any spontaneous symmetry breaking. However, CDW order is also present due to correlations, and the fact that it is energetically favorable, $\delta^2 E \sim t^2/U$, to have doubly occupied and empty sites adjacent.

Additional interest in the orbital occupation evolution concerns its possible implications for charge transfer processes in cuprate pairing. Because they favor d-wave pairing symmetry, it is generally accepted that spin fluctuations provide the majority of the "pairing glue" in high T_c materials [38]. However, arguments have been made [3–8] in favor of a possible role of charge fluctuations between the copper and oxygen orbitals driven by a repulsive interaction V_{pd}. Such fluctuations would be reflected in a large response of $n_p - n_d$ to the orbital energy difference $\epsilon_p - \epsilon_d$. Figure 2 emphasizes that, even in the absence of V_{pd}, there is nontrivial structure in the orbital occupations. Thus, much as the large $U = 0$ antiferromagnetic susceptibility highlights spin fluctuations on the square lattice, the observation of unusual charge transfer in the Lieb lattice at $V_{pd} = 0$ might indicate a role for charge fluctuations there.

Because it probes the double occupancy D (local pair formation), the local moment can also provide interesting insight. $\langle m^2 \rangle = \rho - 2D$ is shown in Fig. 3. It is evident that $\langle m^2 \rangle$ does not change as the density is increased in the range $2/3 < \rho < 4/3$, i.e., as the flat band is being filled. This result can be understood within MFT: for chemical potential $\mu = 0$, the SU(2) invariance implies that the mean field ground state energy is invariant under a global rotation of the mean field pseudospins $\langle \vec{\Delta}_i \rangle$. More precisely, in the ground state, $\langle \vec{\Delta}_i \rangle$ shows a ferromagnetic order in the (X, Y) plane (pairing order) and an antiferromagnetic order along the Z axis (CDW order).

This SU(2) symmetry implies

$$\frac{P_s}{a} + \left(\frac{\rho - 1}{b}\right)^2 = 1, \tag{3}$$

where $9a = (2\Delta_p + \Delta_d)^2$ and $3b = 4\Delta_p - 2\Delta_d$, and $\Delta_i = |\langle \vec{\Delta}_i \rangle|$ is the norm of the pseudospin. The maximum value for P_s is a and occurs at half filling; P_s vanishes when the density reaches $\rho = 1 \pm b$. At $U = -4$, the numerical MFT values are $\Delta_d = 0.1876$ and $\Delta_p = 0.3438$, with $a \approx 0.09$ and $b = 1/3$. Although the maximum value of P_s depends on U, we have found that the value of b is always $1/3$. Hence, for $\mu = 0$, the mean field P_s always vanishes at fillings $\rho = 1 \pm 1/3$, i.e., the endpoints of the flat band, in agreement with the QMC results [39] depicted in Fig. 5. Finally, one has $(n_\uparrow - n_\downarrow)^2 = 1 - 4\vec{\Delta} \cdot \vec{\Delta}/3$. Since, at the mean-field level, $|\langle \vec{\Delta} \rangle|^2$ is independent of the density within the range $2/3 < \rho < 4/3$, this explains the plateau in Fig. 3. It is remarkable that this behavior is observed in the QMC results (Fig. 3) as, in the exact Hamiltonian, the SU(2) symmetry is only present at $\rho = 1$ or $\mu = 0$ and not in the whole range of densities $2/3 < \rho < 4/3$.

B. Competition between pairing and charge order

Nearest-neighbor density-density correlations (Fig. 4) involving a copper site occupation $\langle n^d n^{px} \rangle$ decrease with increasing ρ in the flat band, reflecting the transfer of charge to the oxygen sites. The density correlations between the two oxygen sites of a unit cell, $\langle n^{px} n^{py} \rangle$, grow with filling. The anomalous charge response is strengthened as the on-site interaction strength $|U|$ becomes larger.

The pair structure factor in the intermediate coupling regime, $U = -4$, is given in Fig. 5 (top). P_s is greatest when the bands are half filled, i.e., for $\rho = 1$ and $\rho = 5/3$. These

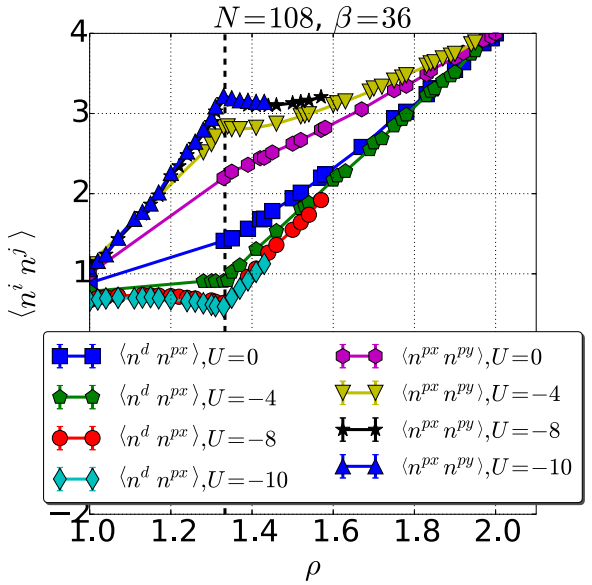

FIG. 4. (Color online) Near-neighbor and next near-neighbor density-density correlations as functions of ρ for $U = 0, -4, -8, -10$. As with the site occupations, these short range density correlations exhibit an anomalous decrease even as the total density ρ grows.

densities are furthest from the fillings $\rho = 2/3$ and $\rho = 4/3$ which most favor competing CDW phases [Figs. 1(b) and 1(c)] and, therefore, vanishing P_s. (P_s also vanishes at full filling, $\rho = 2$.) Data for P_s do not show much size dependence for $U = -4t$. Inset (a) to Fig. 5 gives a finite size scaling analysis [40] and supports the existence of pairing LRO in the thermodynamic limit $1/L \to 0$ as expected in two dimensions in the zero temperature limit. For the finite size systems we are using this limit is reached when the coherence length becomes larger than the system's size. This result is in agreement with the mean field results: For $1 \leqslant \rho \leqslant 4/3$, the mean field pair structure factor is given by $P_s = P_s^{\max}(1 - [3(\rho - 1)]^2)$, where $P_s^{\max} = 0.09$, in very good agreement with the QMC. For $4/3 \leqslant \rho \leqslant 2$, the mean field results also depict a dome-shape behavior, with a maximum around the center, a behavior quite similar to a single-band situation. The agreement between MFT and DQMC is less good at larger $|U|$.

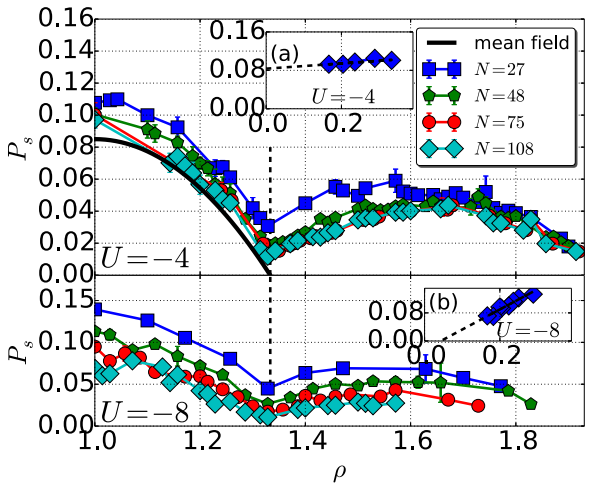

FIG. 5. (Color online) Pair structure factor P_s versus ρ for $U = -4t$ (top) and $U = -8t$ (bottom). Data for four lattice sizes are shown. P_s has a minimum at $\rho = 4/3$ where the superconducting phase must compete with charge order and a maximum when $\rho = 1$ and $\rho = 5/3$. In the weaker coupling case $U = -4t$, at half filling (inset a) P_s extrapolates to a nonzero value in the thermodynamic limit. However, at $U = -8t$, the extrapolation is to zero (inset b). For $1 \leqslant \rho \leqslant 4/3$, the mean field pair structure factor is given by $P_s = P_s^{\max}(1 - [3(\rho - 1)]^2)$, where $P_s^{\max} = 0.09$, in very good agreement with the QMC results. For $4/3 \leqslant \rho \leqslant 2$, the mean field calculations depict a similar dome-shape behavior, with a maximum around the center, a behavior quite similar to a single-band situation.

C. BEC within a flat band

The bottom panel of Fig. 5 shows DQMC data at larger $U = -8t$, approaching the small pair size regime of the AHM. P_s decreases much more as the lattice size is increased than for $U = -4t$, and a finite size scaling analysis [inset (b)] suggests the absence of LRO at $\beta = 36$. We thus have local pair formation with no clear long range coherence. While LRO pair order is likely to develop at a yet lower energy scale, it is suggestive that it is absent at temperatures for which superconductivity would be readily visible in dispersing band geometries like the 2D square lattice: The flat band appears to be impeding the bosons (locally formed pairs) from forming a BEC. For $U = -8t$, pairing LRO is well established at $\beta = 12$ on a square lattice. In the flat-band model considered here, $\beta = 36$ is insufficiently cold. This factor of three, or more, reduction in the ordering temperature is much larger than one

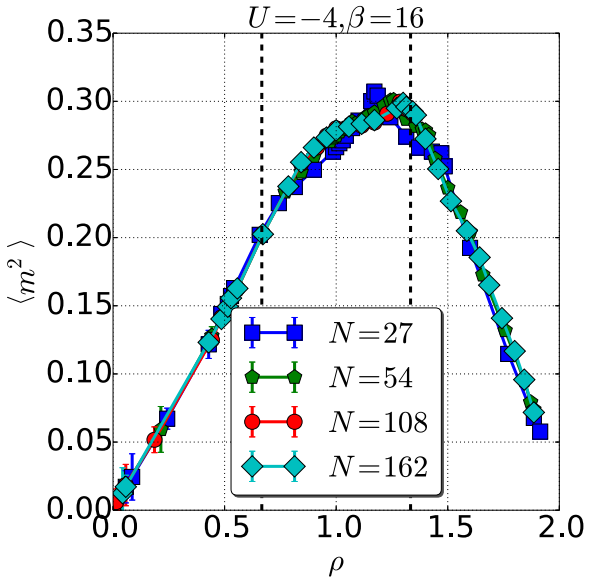

FIG. 6. (Color online) Local magnetic moment versus ρ for the Kagome lattice at $U = -4$. Dashed lines show the noninteracting limit between the three bands, the lowest energy band being flat. The magnetic moment is approximately proportional to the density ρ in the flat band. Unlike the Lieb case, there is no signature in this quantity as the boundary from the flat band to the second, dispersing, band is crossed.

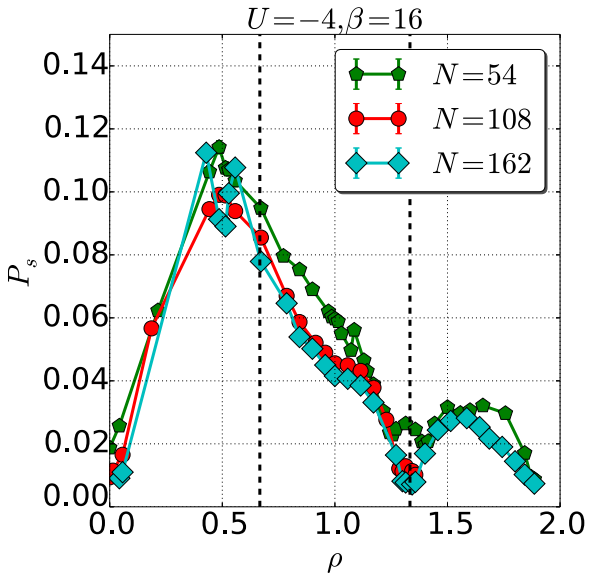

FIG. 7. (Color online) Pair structure factor P_s versus ρ for the Kagome lattice at $U = -4$. As for the magnetic moment (Fig. 6), we do not observe a peculiar behavior in the flat-band region.

would expect simply by the lower coordination number (4 for the square lattice and 8/3, on average, for the CuO_2 lattice).

D. Comparison with the Kagome lattice

In order to assess if these phenomena are generic to all flat-band geometries, we compare our results with the case of the Kagome lattice. We choose the sign of the hopping term so that the dispersionless band is the lowest of the three Kagome bands. This is the case of interest to proposed optical lattice experiments on BEC in Kagome lattices [30], since condensation occurs at the lowest energy levels.

Figures 6 and 7 shows the evolution of the local magnetic moment $\langle m^2 \rangle$ and the pair structure factor P_s for $U = -4$ and different lattice sizes. In the noninteracting limit, the flat band is occupied for density $\rho < 2/3$. We see that the features that were observed in the Lieb lattice (Figs. 3 and 5) are no longer present. Specifically, the local moment $\langle m^2 \rangle$ is not constant, nor does the pair structure factor P_s become zero at the edge of the flat band. This reflects the absence of competition between CDW and SC order in the Kagome case. Moreover, we do not observe a sharp change in the behavior of either of these observables when the system transitions from the first to the second band. There are, however, signatures as the density takes the Fermi level from the second to the third band, both of which have nonzero width. This occurs at $\rho \simeq 4/3$. The evolution of P_s and $\langle m^2 \rangle$ at low density is not peculiar; indeed it is the one observed in most cases, with P_s and $\langle m^2 \rangle$ roughly proportional to ρ. We observe a similar behavior in the low or high density limit for the Lieb lattice (see Figs. 3 and 5).

This comparison between the Lieb and Kagome lattices emphasizes that peculiar behavior, like constant magnetization, observed in the Lieb case cannot be ascribed solely to a flat band. In the presence of interactions, there is no generic evolution of magnetic and pairing correlations within a flat band. Instead, other features of the geometry, such as the presence or absence of frustration, of particle-hole symmetry, or the existence of distinct types of sites in the unit cell, also come into play.

IV. CONCLUSIONS

Charge and pair correlations in the AHM in the Lieb lattice, which has a flat band, have been computed. As the flat band is filled, the density on the minority ("copper") sites declines even though the total density grows, demonstrating a specific model in which charge transfer signatures are strong. Such behavior has attracted interest in the context of cuprate superconductivity and materials like $BaPbBiO_3$, where it has been proposed that the exchange of charge fluctuations can mediate pairing in a way analogous to the exchange of spin fluctuations [41]. We have also presented detailed data on the competition between the pairing and CDW response as the density is tuned. At stronger values of the attraction, pairing correlations decrease significantly as the lattice size increases, suggesting that LRO is inhibited by the flat-band dispersion relative to strongly dispersing bands. Finally we compared our results to the Kagome lattice, another example of a flat-band geometry, and showed that the phenomena observed are not generically present in all flat-band systems. Together, these results characterize "traditional" charge and pairing correlations, forming a useful context to attempts to explore more exotic topological phases in flat-band systems.

ACKNOWLEDGMENTS

Work supported by the UCOP, by NNSA-DE-NA0001842-0, by NSF-PIF-1005503, by the CNRS(France)-UC Davis EPOCAL LIA joint research grant and by the CNRS-CQT LIA FSQL.

[1] J. E. Hirsch and D. J. Scalapino, Phys. Rev. Lett. **56**, 2732 (1986).
[2] D. J. Scalapino, E. Loh, and J. E. Hirsch, Phys. Rev. B **35**, 6694 (1987).
[3] V. J. Emery, Phys. Rev. Lett. **58**, 2794 (1987).
[4] C. M. Varma, S. Schmitt-Rink, and E. Abrahams, Solid State Commun. **62**, 681 (1987).
[5] J. Zaanen, G. A. Sawatzky, and J. W. Allen, Phys. Rev. Lett. **55**, 418 (1985).
[6] A. M. Olés and J. Zaanen, Phys. Rev. B **39**, 9175 (1989).
[7] R. T. Scalettar, D. J. Scalapino, R. L. Sugar, and S. R. White, Phys. Rev. B **44**, 770 (1991).
[8] M. H. Fischer and E.-A. Kim, Phys. Rev. B **84**, 144502 (2011).
[9] E. H. Lieb, Phys. Rev. Lett. **62**, 1201 (1989).
[10] Bill Sutherland, Phys. Rev. B **34**, 5208 (1986).
[11] C. M. Varma, Phys. Rev. B **73**, 155113 (2006).
[12] N. Goldman, D. F. Urban, and D. Bercioux, Phys. Rev. A **83**, 063601 (2011).
[13] M. Nita, B. Ostahie, and A. Aldea, Phys. Rev. B **87**, 125428 (2013).

[14] C. Weeks and M. Franz, Phys. Rev. B **82**, 085310 (2010).
[15] W.-F. Tsai, C. Fang, H. Yao, and J. P. Hu, arXiv:1112.5789.
[16] D. Leykam, O. Bahat-Treidel, and A. S. Desyatnikov, Phys. Rev. A **86**, 031805(R) (2012).
[17] K. Sun, Z.-C. Gu, H. Katsura, and S. Das Sarma, Phys. Rev. Lett. **106**, 236803 (2011).
[18] S. Yang, Z.-C. Gu, K. Sun, and S. Das Sarma, Phys. Rev. B **86**, 241112(R) (2012).
[19] C. Wu and S. Das Sarma, Phys. Rev. B **77**, 235107 (2008).
[20] C. Wu, D. Bergman, L. Balents, and S. Das Sarma, Phys. Rev. Lett. **99**, 070401 (2007).
[21] J. Everts, M.S. thesis, Utrecht University, 2012 and references cited therein.
[22] A. Yamada, K. Seki, R. Eder, and Y. Ohta, Phys. Rev. B **83**, 195127 (2011).
[23] Kai Sun, Hong Yao, Eduardo Fradkin, and Steven A. Kivelson, Phys. Rev. Lett **103**, 046811 (2009).
[24] S. D. Huber and E. Altman, Phys. Rev. B **82**, 184502 (2010).
[25] N. B. Kopnin, T. T. Heikkilä, and G. E. Volovik, Phys. Rev. B **83**, 220503 (2011).
[26] N. B. Kopnin, M. Ijäs, A. Harju, and T. T. Heikkilä, Phys. Rev. B **87**, 140503 (2013).
[27] Shizhong Zhang, Hsiang-hsuan Hung, and Congjun Wu, Phys. Rev. A **82**, 053618 (2010).
[28] V. Apaja, M. Hyrkäs, and M. Manninen, Phys. Rev. A **82**, 041402 (2010).
[29] R. Shen, L. B. Shao, B. Wang, and D. Y. Xing, Phys. Rev. B **81**, 041410 (2010).
[30] D. M. Stamper-Kurn (private communication).
[31] For a review, see M. Randeria and E. Taylor, Ann. Rev. Conden. Matter Phys. **5**, 209 (2014) and references cited therein.
[32] In a three-band model of CuO_2 planes, a site energy difference $\epsilon_p - \epsilon_d > 0$ ensures holes preferentially occupy Cu d orbitals, as occurs in the cuprates. Lieb's theorems do not apply in the presence of such a term, which also would create a sign problem in QMC [33], so we do not include it.
[33] E. Y. Loh, J. E. Gubernatis, R. T. Scalettar, S. R. White, D. J. Scalapino, and R. L. Sugar, Phys. Rev. B **41**, 9301 (1990).
[34] R. Blankenbecler, D. J. Scalapino, and R. L. Sugar, Phys. Rev. D **24**, 2278 (1981).
[35] S. R. White, D. J. Scalapino, R. L. Sugar, E. Y. Loh, Jr., J. E. Gubernatis, and R. T. Scalettar, Phys. Rev. B **40**, 506 (1989).
[36] Trotter errors from the discretization of the inverse temperature are less than a few percent and are smaller than statistical error bars in the structure factors.
[37] J. Minar and B. Grémaud, Phys. Rev. B **88**, 235130 (2013).
[38] D. J. Scalapino, in *Proceedings of the International School of Physics*, edited by R. A. Broglia and J. R. Schrieffer (North-Holland, New York, 1994), and references cited therein.
[39] A similar analysis on the square lattice would lead to vanishing b coefficient such that $\mu = 0$ only corresponds to half filling.
[40] D. A. Huse, Phys. Rev. B **37**, 2380 (1988).
[41] N. E. Bickers, D. J. Scalapino, and R. T. Scalettar, Int. J. Mod. Phys. B **1**, 687 (1987).